Next generation redshift surveys and the origin of cosmic acceleration

Viviana Acquaviva,* Amir Hajian,+ David N. Spergel,‡ and Sudeep Das§

Department of Astrophysical Sciences, Peyton Hall, Princeton University, Princeton, New Jersey 08544, USA

(Received 14 March 2008; published 7 August 2008)

Cosmologists are exploring two possible sets of explanations for the remarkable observation of cosmic acceleration: dark energy fills space or general relativity fails on cosmological scales. We define a null test parameter $\epsilon(k, a) \equiv \Omega_m^{-\gamma} d\ln D/d\ln a - 1$, where a is the scale factor, D is the growth rate of structure, $\Omega_m(a)$ is the matter density parameter, and γ is a simple function of redshift. We show that it can be expressed entirely in terms of the bias factor, $b(a)$, measured from cross correlations with cosmic microwave background (CMB) lensing, and the amplitude of redshift-space distortions, $\beta(k, a)$. Measurements of the CMB power spectrum determine $\Omega_{m0}H_0^2$. If dark energy within general relativity is the solution to the cosmic acceleration problem, then the logarithmic growth rate of structure $d\ln D/d\ln a = \Omega_m^\gamma$. Thus, $\epsilon(k, a) = 0$ on linear scales to better than 1%. We show that in the class of modified gravity models known as $f(R)$, the growth rate has a different dependence on scale and redshift. By combining measurements of the amplitude of β and of the bias, b, redshift surveys will be able to determine the logarithmic growth rate as a function of scale and redshift. We estimate the predicted sensitivity of the proposed SDSS III (BOSS) survey and the proposed ADEPT mission and find that they will test structure growth in general relativity to the percent level.

DOI: 10.1103/PhysRevD.78.043514 PACS numbers: 98.80.Es, 04.50.Kd, 95.36.+x, 98.62.Py

I. INTRODUCTION

In general relativity (GR), there are four variables characterizing linear cosmic perturbations: the two gravitational potentials Ψ and Φ, the anisotropic stress, σ, and the pressure perturbation, δp. All of these variables can depend on the wave number k and the expansion factor a. We focus initially on models with no dark energy clustering or pressure and discuss these effects later in the paper. We assume scalar linear perturbations around a flat Friedmann-Robertson-Walker background in the Newtonian gauge,

$$ds^2 = -(1 + 2\Psi)dt^2 + a^2(1 + 2\Phi)dx^2 \tag{1}$$

and work in the quasistatic, linear approximation, which is valid for subhorizon modes still in the linear regime.

The evolution of perturbations is described by the continuity, Euler and Poisson equations (i.e. [1]):

$$\Delta_m' = -k_H V_m, \tag{2}$$

$$V_m' + V_m = \frac{k}{aH}\Psi, \tag{3}$$

$$k^2\Phi = -4\pi G a^2 \rho_m \Delta_m. \tag{4}$$

With the assumption of no anisotropic stress, $\Phi = -\Psi$, these equations can be combined to derive the equation of motion for the growth factor D, defined as $D(k, z) = \delta_m(k, z)/\delta_m(k, z = \infty)$:

$$D'' + \left(2 + \frac{H'}{H}\right)D' - \frac{4\pi G}{H^2}\rho_m D = 0; \tag{5}$$

where $H = \dot{a}/a$ is the Hubble function, and a prime denotes the derivative with respect to $\ln a$. From Eq. (5) one can infer the two key features of GR with smooth dark energy. First, the growth factor is exactly determined once the Hubble function $H(a)$ is known; and second, since none of the coefficients is a function of scale, the growth factor is scale independent. Therefore, for a given expansion history, one can test GR in two ways: checking that the theoretical solution of Eq. (5) agrees with observations, and testing the hypothesis of scale independence [2–11]. The growth rate of structure in GR is well approximated by Ω_m^γ, where the fitting function $\gamma(z) \simeq 0.557 - 0.02z$ is accurate at the 0.3% level [12]. We define a function that tests the growth rate of structure and can be directly related to observables:

$$\epsilon(k, a) = \Omega_m^{-\gamma(a)}\frac{d\ln D}{d\ln a} - 1 = \frac{a^{3\gamma}H(a)^{2\gamma}}{(\Omega_{m,0}H_0^2)^\gamma}\frac{d\ln D}{d\ln a} - 1. \tag{6}$$

The combination $\Omega_{m,0}H_0^2$ can be constrained via cosmic microwave background (CMB) measurements; it is currently known to within the 5% level fro the WMAP5 data [13], with an expected gain of a factor $\simeq 4$ from the upcoming satellite CMB mission Planck [14]. The solid line in Fig. 1 shows $\epsilon(a)$ in GR with dark energy: regardless of the details of the dark energy model, $\epsilon(a) \simeq 0$ in the linear regime. By measuring this quantity, we can characterize deviations from general relativity.

*vacquavi@princeton.edu
+ahajian@princeton.edu
‡dns@astro.princeton.edu
§sudeep@astro.princeton.edu

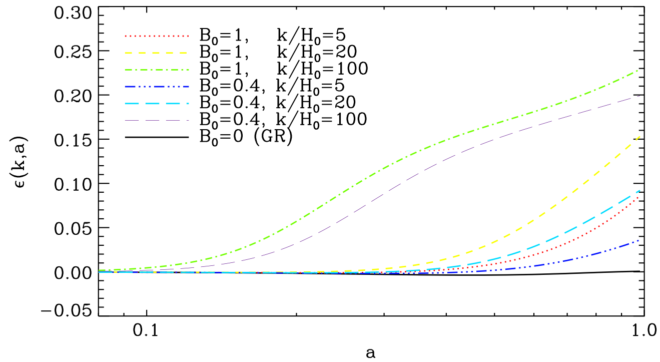

FIG. 1 (color online). The behavior of $\epsilon(k, a) = \Omega_m^{-\gamma} d\ln D/d\ln a - 1$ in GR (solid line) and in $f(R)$ models, as a function of B_0 and k. Growth is enhanced for $B_0 \neq 0$ and at smaller scales in alternative theories. In GR, $\epsilon(a) = 0$.

II. $f(R)$ THEORIES IN THE PARAMETERIZED POST-FRIEDMANN FORMALISM

To quantify the expected deviations, we study a class of modified gravity (MoG) models known as $f(R)$ theories, whose action is written as

$$\mathcal{S} = \frac{1}{16\pi G}\int d^4x\sqrt{-g}(R + f(R)) + \mathcal{S}_m; \tag{7}$$

S_m is the action of standard matter fields. It was noted long ago [15,16] that models where $f(R)$ is an inverse power of the Ricci scalar can give rise to late-time acceleration; however, many of those models have been shown not to be cosmologically viable due to gravitational instability [17].

Recently, Song, Hu, and Sawicki [18] introduced an effective parametrization for $f(R)$ theories which does not rely on any particular model and is able to discard models suffering from instabilities. The cosmological evolution is obtained by fixing the expansion history to match that of a dark energy model, for which we assume a constant equation of state w:

$$H^2 = H_0^2(\Omega_m a^{-3} + (1 - \Omega_m)a^{-3(1+w)}). \tag{8}$$

Such requirement for $H(a)$ translates into a second-order equation for $f(R)$, which can be solved numerically. Of the two initial conditions of this equation, one can be fixed requiring that $f(R)/R \to 0$ at early times (i.e. for large R) in order to recover GR; the second defines a one-parameter family of curves which all generate the given $H(a)$. Such a parameter is conveniently chosen as (also see [19]):

$$B_0 = \left(\frac{f_{RR}}{1 + f_R}R'\frac{H}{H'}\right)_0. \tag{9}$$

Here f_R and f_{RR} represent the first and second derivative of f with respect to R. GR is represented by the special case $B_0 = 0$, so that B_0 effectively quantifies the deviation from GR at the present time. Furthermore, the gravitational stability condition is easily established as $B_0 > 0$.

The additional degrees of freedom of the $f(R)$ gravity introduce modifications in the Poisson equation and in the relation between the two gravitational potentials [1], which now read

$$k^2(\Phi - \Psi) = 4\pi G_{\rm eff}(k, a)a^2\rho_m\Delta_m \tag{10}$$

and

$$\Psi = (g(k, a) - 1)\frac{k}{aH}(\Phi - \Psi). \tag{11}$$

The equation for the growth factor in MoG takes the form

$$D'' + \left(2 + \frac{H'}{H}\right)D' + \frac{4\pi G_{\rm eff}(k, z)(g(k, z) - 1)}{H^2}\rho_m D = 0. \tag{12}$$

Given $H(a)$, a MoG model is not completely defined unless $G_{\rm eff}(k, a)$, the effective Newton's constant, and the metric ratio $g(k, a) = (\Phi + \Psi)/(\Phi - \Psi)$, are known, contrary to the GR case. For the class of $f(R)$ theories under study, and in the subhorizon, linear regime, Hu and Sawicki [20] have provided a fit to $G_{\rm eff}$ and g as

$$\begin{aligned} G_{\rm eff}(k, a) &= G_{\rm eff}(a) = \frac{G_N}{1 + f_R}, \\ g(k, a) &= \frac{g_{\rm SH}(a) - \frac{1}{3}(0.71\sqrt{B}(k/aH))^2}{1 + (0.71\sqrt{B}(k/aH))^2}, \end{aligned} \tag{13}$$

where B is the function appearing in Eq. (9), and $g_{\rm SH}(a)$ is the superhorizon metric ratio (see [18,20] for details). The key result is that the $f(R)$ models all predict an enhancement in the growth rate of structure. In fact, any positive value of B_0 gives rise to a negative f_R, so that the effective Newton constant is larger with respect to GR. Moreover, both terms in $g(k, a)$ have a negative sign, which induce further enhancement of matter clustering, as can be seen from Eq. (12). Since $G_{\rm eff}(k, z) = G_N/(1 + f_R)$ does not depend on k, the scale dependence of the growth factor can only arise from the second term of Eq. (13). On large scales, the dominant term in the metric ratio is $g_{\rm SH}(a)$, while for increasing values of k, the second term in the expression for $g(k, a)$ becomes important and tends to the constant value of $-1/3$ for large k. The scale of the transition from scale-free to scale-dependent growth factor is $k/aH \simeq B^{-1/2}$; due to the asymptotic behavior of $g(k, a)$, the growth differs significantly from GR even for models with very small values of B_0, on sufficiently small scales. A mechanism to restore GR on scales of the galaxy and smaller is discussed in [20,21]. Figure 1 shows $d\ln(D)/d\ln(a)\Omega_m(a)^\gamma - 1$ for a few different values of B_0 and k/aH_0. For the GR case, $B_0 = 0$, $\epsilon(k, a) - 1 \simeq 0$ with no scale dependence.

III. MEASURING THE GROWTH OF STRUCTURE

Peculiar velocities displace galaxies along the line of sight in redshift space and distort the power spectrum of galaxies observed in redshift space. This effect is known as linear redshift-space distortion and was first derived by Kaiser [22]. In redshift space, the power spectrum is amplified by a factor $(1+\beta\mu_{\mathbf{k}}^2)^2$ over its real-space counterpart,

$$P^s(\mathbf{k}) = (1+\beta\mu_{\mathbf{k}}^2)^2 P(k), \tag{14}$$

where $P^s(\mathbf{k})$ and $P(k)$ are redshift and real space power spectra, respectively, $\mu_{\mathbf{k}} = \hat{z}\cdot\hat{k}$ is the cosine of the angle between the wave vector $\hat{k}$ and the line of sight $\hat{z}$, and β is the linear redshift-space distortion parameter defined as

$$\beta(a) = \frac{1}{b}\frac{d\ln D}{d\ln a}; \tag{15}$$

b is the linear bias, which we assume to be independent of scale.

Galaxy redshift surveys can be used to directly measure β, and, if the bias is known, the growth rate of perturbations. In fact, the redshift-space power spectrum can be decomposed into harmonics, whose relative amplitude depend on the growth rate of structure through β. The possibility of using such dependence in order to constrain dark energy properties has been explored in [23]; here we focus on the measurements of the scale dependence of β as a smoking gun of modified gravity.

We assume that β is obtained through the ratio of quadrupole to monopole moments of the redshift power spectrum [24]

$$\frac{P_2(k)}{P_0(k)} = \frac{\frac{4}{3}\beta + \frac{4}{7}\beta^2}{1+\frac{2}{3}\beta+\frac{1}{5}\beta^2}, \tag{16}$$

and use the prescription in [25] to get the errors in the above quantities:

$$\frac{\sigma(P_i(k))}{P_i(k)} = \left(\frac{(2\pi)^3\int d^3\mathbf{r}\bar{n}^4(\mathbf{r})\psi^4(\mathbf{r})[1+\frac{1}{\bar{n}(\mathbf{r})P_i(k)}]^2}{V_k[\int d^3\mathbf{r}\bar{n}^2(\mathbf{r})\psi^2(\mathbf{r})]^2}\right)^{1/2}, \tag{17}$$

where $\bar{n}(\mathbf{r})$ is the mean galaxy density, ψ is the weight function, V_k is the volume of the shell in k space, and the index "i" assumes the values 0 and 2 for monopole and quadrupole, respectively.

The linear bias for a population of large-scale structure tracers can be estimated by cross-correlating the line-of-sight projected density of the tracer with a convergence map reconstructed by CMB-lensing techniques and comparing the resulting signal with theory. The weak lensing potential responsible for lensing the CMB can be written as the line-of-sight integral [26],

$$\phi(\hat{\boldsymbol{n}}) = -\int d\eta \frac{d_A(\eta_0-\eta)}{d_A(\eta_0)d_A(\eta)}[\Phi-\Psi](d_A(\eta)\hat{\boldsymbol{n}},\eta), \tag{18}$$

where $d_A(\eta)$ is the comoving angular diameter distance corresponding to the comoving distance η, and η_0 is the comoving distance to the last scattering surface. A quadratic combination of the measured CMB temperature and polarization [27–29] provides an estimator of the convergence field, $\kappa = \frac{1}{2}\nabla^2\phi$. In this study, we have used the prescription of [27] to compute the expected noise power spectrum, $N_\ell^{\kappa\kappa}$, corresponding to the reconstructed convergence field by cross-correlating κ with the projected fractional overdensity of the tracer,

$$\Sigma(\hat{\boldsymbol{n}}) = \int d\eta W(\eta) b\delta_m(\eta\hat{\boldsymbol{n}},\eta), \tag{19}$$

where W is the normalized tracer distribution function in comoving distance. We measure the cross correlation spectrum:

$$C_\ell^{\kappa-\Sigma} = \frac{3}{2}b\Omega_m H_0^2\int d\eta\frac{W(\eta)}{a(\eta)}P\left(\frac{\ell}{d_A},\eta\right)\frac{d_A(\eta_0-\eta)}{d_A(\eta)d_A(\eta_0)}, \tag{20}$$

where $P(k,\eta)$ is the matter power spectrum at the comoving distance η and we have related the wave number k to the multipole ℓ via the Limber approximation [30]. The signal-to-noise ratio for such a cross correlation can be estimated as [31],

$$\left(\frac{S}{N}\right)^2 = f_{\rm sky}\sum(2\ell+1)\frac{(C_\ell^{\kappa-\Sigma})^2}{(C_\ell^{\kappa\kappa}+N_l^{\kappa\kappa})(C_\ell^{\Sigma\Sigma}+N_\ell^{\Sigma\Sigma})}, \tag{21}$$

where $f_{\rm sky}$ is the fraction of sky over which the cross correlation is performed. For tracer counts the noise is Poisson, and the power spectrum is given by $N_\ell^{\Sigma\Sigma} = 1/\hat{n}$, where $\hat{n}$ is the number of tracer objects per steradian.

TABLE I. Predictions for the errors on bias from the cross correlation studies described in the text. For each combination of experiments, we display the number of galaxies per square degree ($\bar{n}$); the area of overlap (A), the signal-to-noise ratio with which the cross correlation of tracer surface density with CMB lensing can be extracted, (S/N), and the percentage error in the bias, b, for the tracer.

Galaxy Survey	$\hat{n}$	$A/10^3$	z_c	b	CMB Expt.	(S/N)	$\Delta b/b$ (%)
					PLANCK	5.8	17.3
SDSSLRG	12.4	3.8	0.31	2	PACT	11.4	8.8
					IDEAL	20.4	4.9
					PLANCK	10.8	9.3
BOSS1	40.	10	0.3	2	PACT	25.5	3.9
					IDEAL	52.5	1.9
					PLANCK	17.0	5.9
BOSS2	110.	10	0.6	2	PACT	39.4	2.5
					IDEAL	78.2	1.3
					PLANCK	52.8	1.9
ADEPT	3500	27	1.35	1	PACT	107.5	0.9
					IDEAL	228.3	0.4

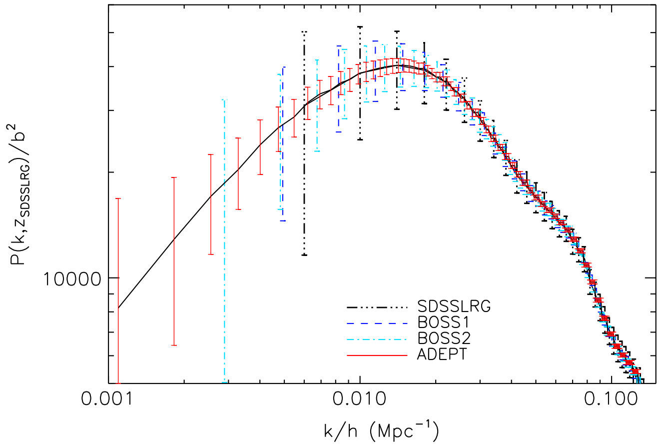

FIG. 2 (color online). Errors on $P(k)$, normalized to the SDSS-LRG median redshift (z = 0.31) for all surveys.

Since the signal is proportional to the bias, b, the expected error on b can be written as

$$\Delta b/b \simeq 1/(S/N). \tag{22}$$

We consider three present and forthcoming redshift galaxy surveys: the SDSS-LRG (Sloan Digital Sky Survey-Luminous Red Galaxies) sample [32], its extension BOSS-LRG (Baryon Oscillation Spectroscopic Survey) [33], which we divide in two redshift bins, labeled as BOSS1 and BOSS2, and the proposed survey ADEPT (Advanced Dark Energy Physics Telescope) [34]. Specifics of each experiment are listed in Table I. In all cases we assume that β and b do not change significantly with redshift within a survey, so that the observed quantity is $\beta(k, z_c)$, where z_c is roughly the central redshift of the survey. As a direct comparison of the capabilities of the three galaxy surveys under examination, we show the real-space matter power spectrum, normalized to the SDSS-LRGs median redshift, with its error bars in Fig. 2. We also consider three possible CMB experiments: a PLANCK-like CMB experiment with 65% sky coverage and temperature and polarization sensitivities of 28 μK arcmin and 57 μK arcmin, respectively; a next generation CMB survey based on using a camera similar to that on ACT (Atacama Cosmology Telescope) or SPT (South Pole Telescope) with a polarimeter and a ~3 years observing program (labeled PACT) with 65% sky coverage and temperature and polarization sensitivities of 13 μK arcmin and 18 μK arcmin, and an ideal polarization experiment (labeled IDEAL) with 65% sky coverage and temperature and polarization sensitivities of 1 μK arcmin and 1.4 μK arcmin, respectively. The expected results from cross correlation with the ADEPT and BOSS surveys, and the SDSS LRG are displayed in Table I.

IV. RESULTS

We show our main results in Fig. 3. Error bars are computed using Planck as the complementary CMB-

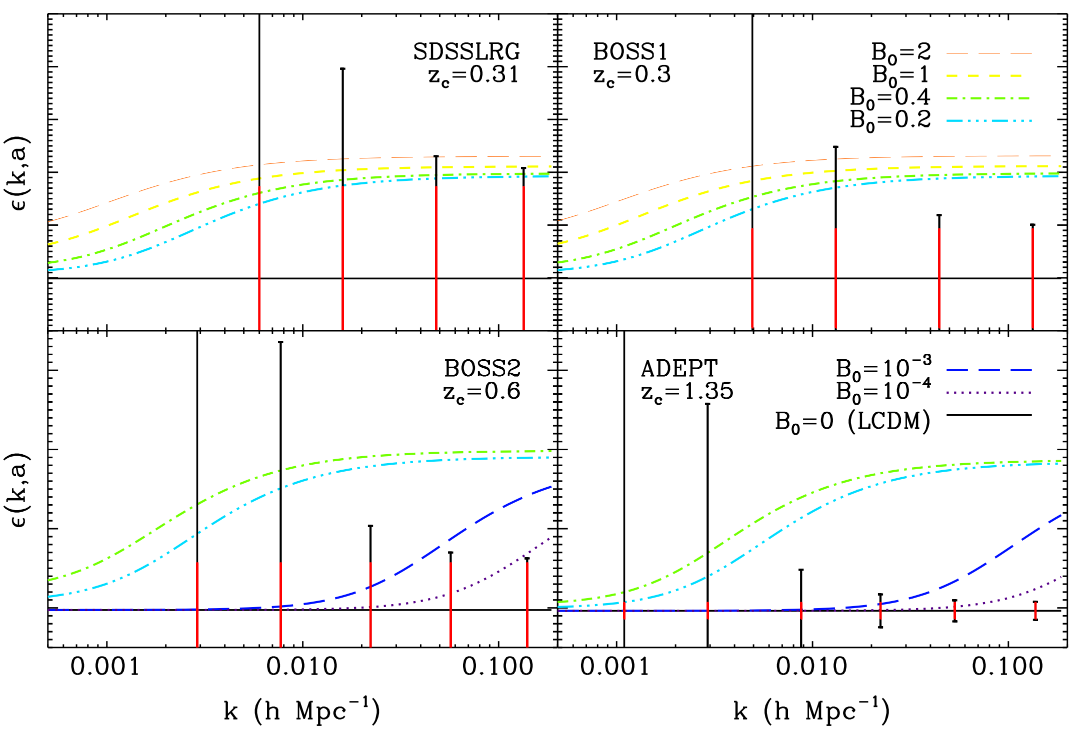

FIG. 3 (color online). $\epsilon(k, z)$ for the four surveys, as a factor of B_0 and k. Total error bars around the ΛCDM case are shown in black; the smaller (red) error bars are from bias only.

TABLE II. Currently available data for measurements of ϵ through β and b (from [35], with the addition of the measurement reported in [23]) and comparison with our predictions. Only the error coming from uncertainties in β and b is considered.

z	β	b	$\Delta\epsilon/\epsilon$ (%)	Ref.	z	$\Delta\epsilon/\epsilon$ (%) $k = 0.05\ h/\mathrm{Mpc}$	$\Delta\epsilon/\epsilon$ (%) $k = 0.2\ h/\mathrm{Mpc}$	Combination of surveys
0.15	0.49 ± 0.09	1.04 ± 0.11	21.5	[36,37]	0.3	22.0	10.1	BOSS1 + Planck
0.35	0.31 ± 0.04	2.25 ± 0.08	25.7	[32]	0.31	39.5	21.0	SDSS LRG + Planck
0.55	0.45 ± 0.05	1.66 ± 0.35	24.0	[38]	0.5	9.3	5.5	BOSS + Planck
0.77	0.70 ± 0.26	1.3 ± 0.1	39.6	[23]	0.6	10.6	6.5	BOSS2 + Planck
1.4	$0.60^{+0.14}_{-0.11}$	1.5 ± 0.20	27.7	[39]	1.35	2.1	1.1	ADEPT + PACT
3.0	$\cdots$	$\cdots$	19.9	[40]				

lensing survey for SDSS LRG and BOSS, and PACT for ADEPT. We summarize the current status of β and bias measurements in Table II and add the expected error bars on ϵ at two different scales, $k/h = 0.05\ \mathrm{Mpc}^{-1}$ and $k/h = 0.2\ \mathrm{Mpc}^{-1}$, from our analysis, for comparison.

The errors on bias are scale independent and vary from 17% for SDSS LRG to $\sim$1% for ADEPT. Errors on β depend on scale; we bin our simulated data in bins in k space of width $\Delta \ln k = 1/e$, and see that for all surveys error bars decrease as we go to smaller scales. The corresponding constraints on ϵ are as strong as a few percent for BOSS, and of the order of 1% for ADEPT.

The combined effect of smaller errors and of the asymptotic behavior of the growth factor, which induces a large deviation of $\epsilon(k, a)$ from its GR value on small scales, is that redshift galaxy surveys are more sensitive to the small-scale modification of gravity than to the large-scale one. Ultimately, the smallest observable value of B_0 will not be set by the capabilities of the survey, but by the breakdown of the linear regime assumption. Assuming $k \simeq 0.05\ \mathrm{Mpc}^{-1}$ as an upper limit, and for values of aH corresponding to redshifts between 0 and 2, the smallest B_0 inducing scale-dependent growth is $B_0 \simeq 10^{-4}$. Such value is within reach of ADEPT; future experiments that detect redshifted 21-cm emission could probe even larger values of k/aH in the linear regime.

V. CONCLUSIONS AND DISCUSSION

We have built a null test parameter for general relativity, $\epsilon(k, a)$, based on the consistency between expansion history and structure growth expected in GR. Such a parameter can be expressed in terms of the combination $\Omega_{0m}h^2$, probed by the CMB experiments, the linear matter perturbations growth factor, probed by redshift galaxy surveys, and the linear bias, probed by cross correlation of the two. We have predicted the achievable precision in the measurement of $\epsilon(k, a)$ for three redshift galaxy surveys, SDSS LRG, BOSS, and ADEPT, together with Planck and a possible future CMB experiment, PACT. We have interpreted such a result in the context of a one-parameter family of modified gravity theories, known as $f(R)$, which can give rise to cosmic acceleration. In such models, the matter clustering is enhanced on all scales with respect to the GR case, and the enhancement is largest on small scales. We concluded that the peculiar signatures of the $f(R)$ theories will be definitely detectable with a survey like ADEPT.

More generally, any detection of deviation of ϵ from zero that was not due to some observational systematic would be a signature of truly novel physics with enhanced growth, pointing either to non-GR physics or to unexpected properties of dark energy: dark energy models with a non-zero sound speed are characterized by an oscillatory behavior of the growth [41], and scalar field dark energy suppresses growth on large scales [42]. Similarly, massive neutrinos suppress $\epsilon(k, a)$ on scales below the neutrino free streaming scale (see [43] for review).

ACKNOWLEDGMENTS

We warmly thank E. Aubourg, C. Hirata, W. Hu, R. H. Lupton, M. A. Strauss, and L. Verde for useful suggestions. D. N. S thanks the APC in Paris for its hospitality. This work was supported by NSF Grant No. AST-0707731, the NSF PIRE program, and the NASA LTSA program.

[1] B. Jain and P. Zhang, arXiv:0709.2375.
[2] E. Bertschinger and P. Zukin, Phys. Rev. D **78**, 024015 (2008).
[3] E. Bertschinger, Astrophys. J. **648**, 797 (2006).
[4] M. Ishak, A. Upadhye, and D. N. Spergel, Phys. Rev. D **74**, 043513 (2006).
[5] S. F. Daniel, R. R. Caldwell, A. Cooray, and A. Melchiorri, Phys. Rev. D **77**, 103513 (2008).
[6] O. Dore *et al.*, arXiv:0712.1599.
[7] E. V. Linder and R. N. Cahn, Astropart. Phys. **28**, 481 (2007).
[8] P. Zhang, M. Liguori, R. Bean, and S. Dodelson, Phys.

Rev. Lett. **99**, 141302 (2007).
[9] Y. Wang, J. Cosmol. Astropart. Phys. 05 (2008) 021.
[10] V. Sahni and A. Starobinsky, Int. J. Mod. Phys. D **15**, 2105 (2006).
[11] K. Yamamoto, T. Sato, and G. Huetsi, arXiv:0805.4789.
[12] D. Polarski and R. Gannouji, Phys. Lett. B **660**, 439 (2008).
[13] J. Dunkley *et al.* (WMAP Collaboration), arXiv:0803.0586.
[14] Planck Collaboration, arXiv:astro-ph/0604069.
[15] S. M. Carroll, V. Duvvuri, M. Trodden, and M. S. Turner, Phys. Rev. D **70**, 043528 (2004).
[16] S. Capozziello, S. Carloni, and A. Troisi, Recent Res. Dev. Astron. Astrophys. **1**, 625 (2003).
[17] A. D. Dolgov and M. Kawasaki, Phys. Lett. B **573**, 1 (2003).
[18] Y.-S. Song, W. Hu, and I. Sawicki, Phys. Rev. D **75**, 044004 (2007).
[19] A. A. Starobinsky, JETP Lett. **86**, 157 (2007).
[20] W. Hu and I. Sawicki, Phys. Rev. D **76**, 104043 (2007).
[21] W. Hu and I. Sawicki, Phys. Rev. D **76**, 064004 (2007).
[22] N. Kaiser, Mon. Not. R. Astron. Soc. **227**, 1 (1987).
[23] L. Guzzo *et al.*, Nature (London) **451**, 541 (2008).
[24] A. J. S. Hamilton, in *The Evolving Universe*, edited by D. Hamilton (Kluwer, Dordrecht, 1998).
[25] H. A. Feldman, N. Kaiser, and J. A. Peacock, Astrophys. J. **426**, 23 (1994).
[26] M. Bartelmann and P. Schneider, Phys. Rep. **340**, 291 (2001).
[27] W. Hu and T. Okamoto, Astrophys. J. **574**, 566 (2002).
[28] T. Okamoto and W. Hu, Phys. Rev. D **67**, 083002 (2003).
[29] C. M. Hirata and U. Seljak, Phys. Rev. D **67**, 043001 (2003).
[30] D. N. Limber, Astrophys. J. **119**, 655 (1954).
[31] H. V. Peiris and D. N. Spergel, Astrophys. J. **540**, 605 (2000).
[32] M. Tegmark *et al.* (SDSS Collaboration), Phys. Rev. D **74**, 123507 (2006).
[33] Details can be found at www.sdss3.org.
[34] Details can be found at www7.nationalacademies.org/ssb/be_nov_2006_bennett.pdf.
[35] S. Nesseris and L. Perivolaropoulos, Phys. Rev. D **77**, 023504 (2008).
[36] E. Hawkins *et al.*, Mon. Not. R. Astron. Soc. **346**, 78 (2003).
[37] L. Verde *et al.*, Mon. Not. R. Astron. Soc. **335**, 432 (2002).
[38] N. P. Ross *et al.*, arXiv:astro-ph/0612400.
[39] J. da Angela *et al.*, arXiv:astro-ph/0612401.
[40] P. McDonald *et al.* (SDSS Collaboration), Astrophys. J. **635**, 761 (2005).
[41] S. DeDeo, R. R. Caldwell, and P. J. Steinhardt, Phys. Rev. D **67**, 103509 (2003).
[42] S. Unnikrishnan, H. K. Jassal, and T. R. Seshadri, arXiv:0801.2017.
[43] J. Lesgourgues and S. Pastor, Phys. Rep. **429**, 307 (2006).